D6-23716
October 1968

Relationship Between Composition, Microstructure, and Stress Corrosion Cracking in Titanium Alloys

R. E. Curtis

BOEING

COMMERCIAL AIRPLANE DIVISION
RENTON BRANCH

D D C
RECEIVED
APR 9 1969
C

29

RELATIONSHIP BETWEEN COMPOSITION, MICROSTRUCTURE, AND STRESS CORROSION CRACKING IN TITANIUM ALLOYS

By R. E. Curtis

ABSTRACT

Four α titanium alloys and 11 $\alpha+\beta$ titanium alloys have been characterized to relate phase composition and associated microstructure to stress corrosion cracking (SCC). Of these alloys, only a low-interstitial, commercially pure α alloy (Ti-5CA) was immune to SCC. Addition of oxygen, aluminum, or aluminum and tin restricted slip in the α phase and promoted stress corrosion susceptibility. Formation of ordered domains of Ti3(Al,Sn) further restricted slip and increased susceptibility. Stress corrosion resistance was improved by thermomechanical treatments that reduced α grain size or increased dislocation density. Alpha-phase susceptibility is qualitatively related to the intensity of the stress field surrounding a dislocation pileup. Alloying with molybdenum and/or vanadium increased strength and often improved stress corrosion resistance. This is attributed to stabilization of the ductile β phase. However, precipitation of a fine dispersion of α or ω in β caused embrittlement and reduced the stress corrosion threshold. Intermetallic compound formation in alloys containing copper or silicon similarly promoted susceptibility. Thermomechanical processing of Ti-4Al-4Mo-2Sn-0.5Si limited the embrittlement, probably by refining Ti5Si3 particles in the β phase.

INTRODUCTION

Recent tests have demonstrated the susceptibility of numerous titanium alloys to SCC in saltwater environments (1, 2, 3). The results show that neither α, $\alpha+\beta$, nor β alloys are immune to this phenomenon. However, the degree of embrittlement varied markedly within each alloy type.

An extensive evaluation of two $\alpha+\beta$ alloys, Ti-6Al-4V and Ti-4Al-3Mo-1V, showed that differences in susceptibility are partially explained by composition differences (4,5). The additional aluminum in Ti-6Al-4V contributed to extensive slow crack growth in salt solution and reduced the sustained load threshold for SCC. The α phase was identified as the susceptible phase in this alloy, whereas the β phase behaved in a ductile manner, i.e. as a crack arrestor. Because of this difference in the phases, processes that change the amount and morphology of the α and β phases also influence alloy susceptibility. These microstructural changes arise from variations in heat treatment and thermomechanical treatment.

Greater understanding of SCC in titanium alloys requires analysis of a wide spectrum of compositions and associated microstructures. Changes in susceptibility associated with interstitial α stabilizers such as oxygen and with neutral strengtheners such as tin and zirconium have not been established. In addition, the influence of grain size, grain morphology, and dislocation structure on SCC has not been defined as a function of α-phase composition. Four α-type alloys have been selected for investigation of these factors. Additional alloys containing β stabilizers are being characterized to relate SCC to the amount and composition of stabilized β. Both β isomorphous stabilizers (Mo and V) and β eutectoid stabilizers (Fe, Cu, and Si) are being investigated. An initial analysis has been conducted on commercial and near-commercial alloys that provide the desired composition variations. Results of these tests are expected to suggest experimental composition to more clearly define the influence of a particular element or combination of elements, on SCC.

EXPERIMENTAL PROCEDURE

Titanium alloy plate was purchased in the mill-annealed heat-treatment condition in thicknesses of 0.50 inch or greater. Nominal and actual chemical compositions are shown in Table I. The as-received plate was cut into specimen blanks and either heat treated or thermomechanically processed by rolling. Two tensile specimens and five notched bend specimens were machined from each blank so their long dimension was normal to the final plate rolling direction. The notched bend specimen (6) was fatigue cracked in the manner described by B. F. Brown (7) prior to fracture toughness testing in air and stress corrosion testing in 3.5-percent NaCl solution. All tests were conducted at room temperature.

In the fracture toughness test, two specimens per condition were loaded to failure in four-point bending at a gross area stress rate of 1000 psi/sec. Plane-strain fracture toughness K_{Ic} was calculated from the load at which the 5-percent secant modulus intersected the load deflection curve by the method described in Reference 8. Validity of the K_{Ic} determination was limited to conditions where specimen thickness t was equal to or greater than $2.5(K/0.2\text{-percent}$ yield strength)^2.

In the stress corrosion test, three notched bend specimens per condition were immersed in salt solution prior to four-point loading in a hydraulic apparatus (6). Additional Ti-70 specimens were loaded before immersion in salt solution to determine the effect of loading sequence on K_{Iscc}. In both sequences, the first specimen was loaded to an initial stress intensity level K_{Ii} equal to approximately 70 percent of K_{Ic} and held at that level to failure or for a time of at least 6 hours. Load levels for subsequent specimens were selected to establish a curve of K_{Ii} versus time to failure (Figure 1). Visual monitoring of crack growth and examination of the fracture surface (Figure 2) shows the pre-existing crack propagates in salt solution at these low K-levels until it reaches the critical length (corresponding to K_{Ic})
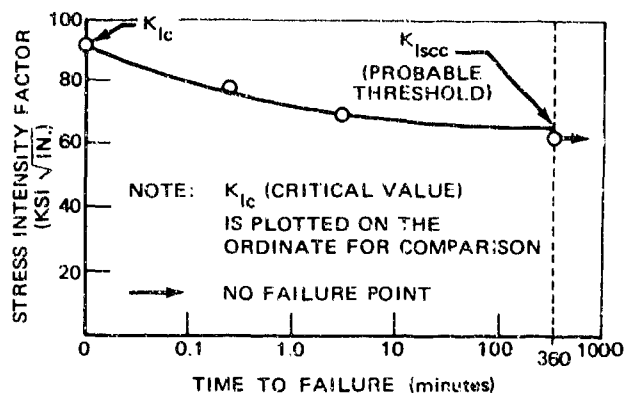

Fig. 1. Typical sustained loading characteristics of titanium alloy plate in salt solution.

necessary for rapid failure. An apparent "threshold level" for stress corrosion cracking exists in titanium alloys below which the pre-existing crack does not grow under sustained load. The threshold is taken as the K_{Ii} level at 360 minutes (Figure 1) and is referred to as K_{Iscc} or "stress corrosion resistance." This value can be compared with the fracture toughness in air K_{Ic} to establish the "relative susceptibility" of each heat-treatment condition.

Samples for microstructure analysis were prepared from broken notched bend specimens. Carbon-germanium replicas of the microstructure and fracture face were prepared using the two-step technique. Coupons for thin foils were machined from the plate midthickness and prepared as described by Blackburn and Williams (9). The volume fraction of beta was determined by the X-ray technique described previously (5).
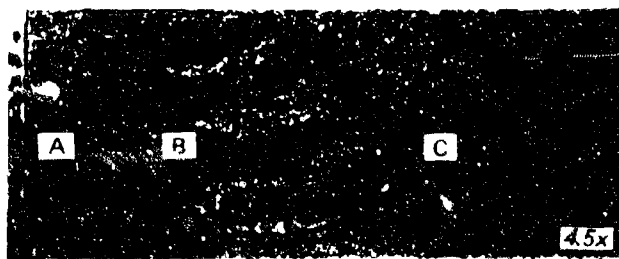

Fig. 2. Fracture surface of notched bend specimen in condition susceptible to stress-corrosion cracking—Area A under the notch is the fatigue-cracked region, area B is the region of slow crack growth in salt solution, and area C is the fast-fracture region.

2

Table I. Composition of titanium alloys.

Alloy	Manufacturer	Heat	Thickness (in.)	Composition (wt %)												
				Al	Sn	Zr	Mo	V	Fe	Cu	Si	W	C	H	O	N
Ti-50A	TMCA	G4832	1.0	—	—	—	—	—	0.10	—	—	—	0.02	0.006	0.12	0.011
Ti-70	Reactive	292206	0.5	—	—	—	—	—	0.38	—	—	—	0.03	0.007	0.38	0.007
Ti-5Al-2.5Sn	Reactive	301064	0.5	5.6	2.6	—	—	—	0.39	—	—	—	0.02	0.007	0.16	0.007
Ti-5Al-5Sn-5Zr	TMCA	D8060	0.5	5.3	5.1	5.3	—	—	0.05	—	—	—	0.02	0.006	0.10	0.011
Ti-2.25Al-11Sn-4Mo-0.2Si (IMI 680)	IMI	AB245	0.5	2.3	10.3	—	4.5	—	0.04	—	0.25	—	0.02	0.003	0.16	0.007
Ti-4Al-3Mo-1V	TMCA	D9484	0.5	4.5	—	—	3.3	1.0	0.10	—	—	—	0.03	0.006	0.11	0.009
Ti-4Al-4Mo-2Sn-0.5Si (Hylite 50)	Jessop-Saville	V.1305	0.63	4.0	2.1	—	4.3	—	0.09	—	0.50	—	0.02	0.005	0.18	0.02
Ti-5Al-3Mo-1V-2Sn	Ore-Met	2536-D1	0.63	5.0	2.0	—	3.0	1.0	0.04	—	—	—	0.01	0.001	0.10	0.02
Ti-6Al-2Mo	Ore-Met	2535-D1	0.63	6.1	—	—	2.0	—	0.06	—	—	—	0.02	0.001	0.11	0.03
Ti-6Al-4V	TMCA	D4988	0.50	6.4	—	—	—	3.9	0.17	—	—	—	0.03	0.003	0.15	0.02
Ti-6Al-6V-2Sn	TMCA	D8058	0.75	5.6	2.1	—	—	5.6	0.82	0.75	—	—	0.02	0.005	0.15	0.02
Ti-6Al-5Zr-1W-0.2Si (IMI 684)	IMI	AC742	1-in. dia	5.75	—	5.1	—	—	0.05	—	0.26	1.0	—	0.003	0.12	—
Ti-7Al-2.5Mo	TMCA	D6860	0.50	6.8	—	—	2.4	—	0.04	—	—	—	0.02	0.004	0.06	0.008
Ti-7Al-4Mo	TMCA	D2735	0.50	6.9	—	—	3.7	—	0.15	—	—	—	0.02	0.005	0.15	0.007
Ti-8Al-1Mo-1V*	—	—	0.50	7.8	—	—	1.0	1.0	0.15	—	—	—	0.02	0.005	0.10	0.008

*Typical composition

3

RESULTS

STRESS-CORROSION
LOADING SEQUENCE

Stress corrosion tests on Ti-70 were conducted using two loading sequences: (1) loading in air before immersion in salt solution, and (2) loading in salt solution. Appendix A shows that the loading sequence had a varied, often pronounced effect on the stress corrosion threshold K_{Iscc}. Of 10 conditions (2A through 2JA) tested with both sequences, eight had a significantly lower threshold when loaded in salt solution. Certain conditions of Ti-6Al-4V behaved similarly (10) However, two of the ten conditions of Ti-70 had identical thresholds for both loading sequences. Ti-8Al-1Mo-1V and Ti-4Al-3Mo-1V also behaved independently of test technique (11). Apparently, conditions that are either markedly susceptible to SCC, e.g. Ti-8Al-1Mo-1V (mill and duplex annealed) and Ti-70 (2D and 2E, Appendix A), or immune to SCC, e.g. Ti-4Al-3Mo-1V, are unaffected by loading sequence. Other alloy conditions, e.g. Ti-6Al-4V and Ti-70 (2A, 2B, 2C, 2F, 2G, 2H, 2I, and 2JA, Appendix A), may exhibit erroneous thresholds if loaded before immersion in salt solution. For this reason, the K_{Iscc} results discussed below were determined from specimens loaded in salt solution.

α ALLOYS

Initial studies have been conducted on four α alloys: a low interstitial grade of commercially pure titanium (Ti-50A, $O_2 = 1200$ ppm), a high interstitial grade of commercially pure titanium (Ti-70*, $O_2 = 3800$ ppm), Ti-5Al-2.5Sn*, and Ti-5Al-5Sn-5Zr. Results of the mechanical-property tests (Appendix A) show that in the as-received (mill annealed) heat-treatment con-

---

*Although Ti-70 and Ti-5Al-2.5Sn are referred to as α alloys, they contain a small amount of β phase in the annealed condition.

dition only Ti-50A is immune to SCC. Immunity is evidenced by a lack of crack growth in salt solution and by the relationship of K_{Ic} to K_{Iscc}. The degree of susceptibility of the other α alloys is dependent on several factors, including (1) grain orientation; (2) composition, order, and dislocation structure; (3) grain size and morphology; and (4) transformation behavior of β, if present. The effect of grain orientation on stress corrosion susceptibility has been discussed previously (12) and will not be considered in detail here.

Composition, Order, and
Dislocation Structure

Increasing the oxygen content of commercially pure titanium and adding aluminum, tin, and zirconium to a commercially pure titanium base stabilized and strengthened the α phase but promoted susceptibility to SCC. Oxygen is responsible for much of the strength difference between Ti-50A (0.2-percent yield = 42.5 ksi) and Ti-70 (0.2-percent yield = 84.3 ksi) in the mill-annealed condition. A portion of the strength increase (approximately 10 ksi) is due to the high iron content of Ti-70 (Table 1) based on Reactive Metals, Inc. data (13).

In addition to strengthening, the increased oxygen in Ti-70 modified the deformation behavior of the α phase so that slip was restricted to a single set of planes, predominately $\{10\bar{1}0\}$. The resulting dislocation structure after 3- to 4-percent deformation by rolling is shown in the electron micrograph in Figure 3(a). Slip on the $\{10\bar{1}0\}$, $\{10\bar{1}1\}$, and (0001) planes in Ti-50A produced dislocation tangles after the same amount of deformation (Figure 3(b)). Operation of three slip systems in Ti-50A is consistent with the results of Churchman (14) who found the critical resolved shear stress for slip on each system to be nearly equal for oxygen levels near 1000 ppm. For lower oxygen levels (100 ppm), slip is preferred on the $\{10\bar{1}0\} <11\bar{2}0>$ system (14). The deformation behavior of Ti-70 suggests that prismatic slip is also preferred for high oxygen levels (3800 ppm).

4
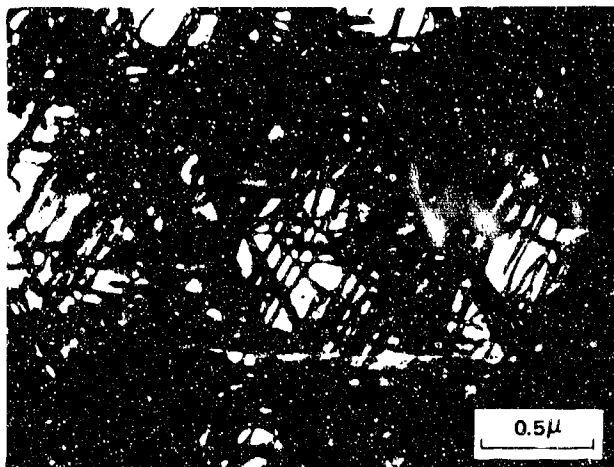
(a)   Ti-70 (oxygen 0.38 wt%).
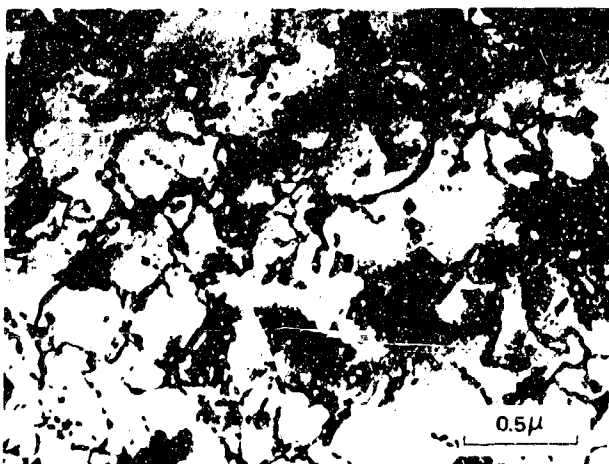
(b)   Ti-50 (oxygen 0.12 wt%)

Fig. 3. Dislocation arrangements after 3% to 4%
          deformation by rolling; [0001] α zone axis.

Fig. 4. Electron fractograph showing cleavage and ductile
          rupture of individual α grains in 3.5% NaCl
          solution, Ti-5Al-5Sn-5Zr, condition 4A — 1650°F/
          1/2 hr/AC.
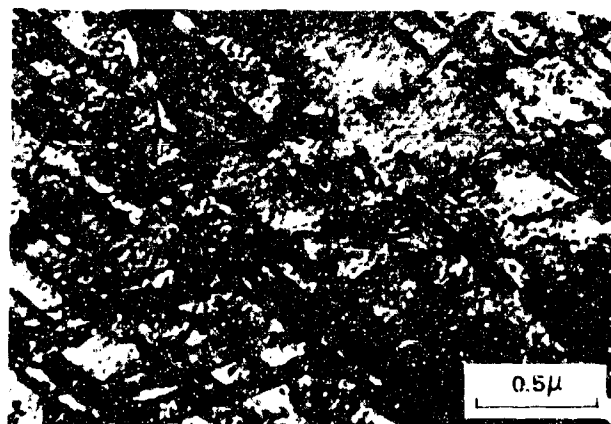
(a)   Disordered, condition 4B — 1650°F/1/2 hr/WQ
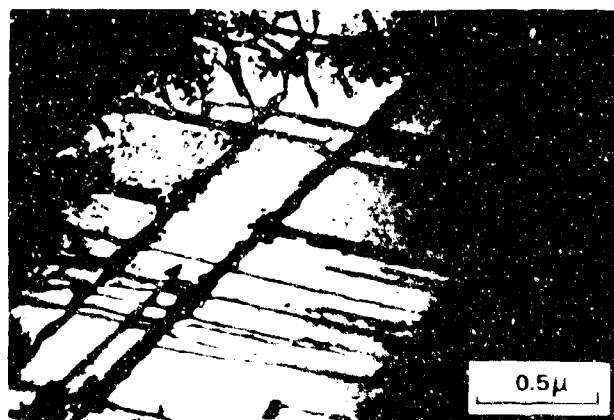
(b)   Ordered, condition 4L — (1650°F/1/2 hr/AC) +
       (1100°F/8hr/FC) to (932°F/120 hr/AC)

Fig. 5. Effect of order on coplanar slip in Ti-5Al-5Sn-5Zr
          deformed 4% in tension, [0001] α zone axis.

Increased oxygen also reduced the applied stress necessary for SCC. In mill-annealed Ti-70 (condition 2A, Table II), environmental crack growth (Figure 2) was observed at K levels as low as 53 ksi $\sqrt{\text{in}}$ compared to $K_c = 114$ ksi $\sqrt{\text{in}}$. Crack growth in the environment occurred by cleavage of individual α grains and by ductile rupture of the remaining grains (Figure 4). Failure in air was by ductile rupture.

Addition of aluminum, tin, and zirconium to an immune, commercially pure base (Ti-50A type) also restricted slip and promoted stress corrosion susceptibility. Thin-foil studies

5

Table II. Strength and fracture properties of ti...
titanium alloys in selected conditions

Alloy & identification	Condition	UTS (ksi)	0.2% yield (ksi)	K_{Ic} (ksi $\sqrt{\text{in.}}$)	K_{Iscc} (ksi $\sqrt{\text{in.}}$)
Ti-50A					
1A	1300°F/1/2 hr/AC	65.8	42.5	60	60
Ti-70					
2A	1300°F/1/2 hr/AC	102.2	84.3	114	54
2E	1500°F/1/2 hr/WQ	106.5	84.6	128	34
2F	(1500°F/1/2 hr/WQ) + (1050°F/1/2 hr/AC)	103.2	82.5	113	39
2G	(1500°F/1/2 hr/WQ) + (1050°F/20 hr/AC)	101.1	82.2	113	33
2H	1700°F/1/2 hr/WQ	100.9	76.5	105	70
Ti-5Al-2.5Sn					
3A	1400°F/2 hr/AC	138.2	129.2	72	26
3C	1650°F/10 hr/AC	132.1	125.1	90	32
3D	1650°F/100 hr/AC (in Argon)	130.3	118.7	92	27
3E	(1400°F/2 hr/AC) + (1100°F/8 hr/FC) to (932°F/120 hr)	139.8	130.5	46	21
3F	1650°F/1 hr/WQ	135.4	124.2	103	27
3H	2000°F/1/2 hr/WQ	140.0	126.6	119	37
Ti-5Al-5Sn-5Zr					
4B	1650°F/1/2 hr/WQ	126.9	109.7	101	67
4D	1850°F/1/2 hr/WQ	136.6	114.1	102	55

AC = air cooled
WQ = water quenched
FC = furnace cooled

6

showed that slip in Ti-5Al-2.5Sn and Ti-5Al-5Sn-5Zr is predominately coplanar. Figure 5(a) illustrates coplanar $\{10\bar{1}0\}$ slip in disordered Ti-5Al-5Sn-5Zr that has been deformed 4.0 percent in tension. Formation of ordered domains of $Ti_3(Al,Sn)$ in this alloy (Figure 6) appeared to reduce the number of operative $\{10\bar{1}0\}$ slip planes and the slip-band thickness (Figure 5(b)). Susceptibility was least pronounced for the disordered solid solution and increased with the degree of order in the α phase. The effect of order on strength, toughness, and stress corrosion resistance is shown in Figure 7.
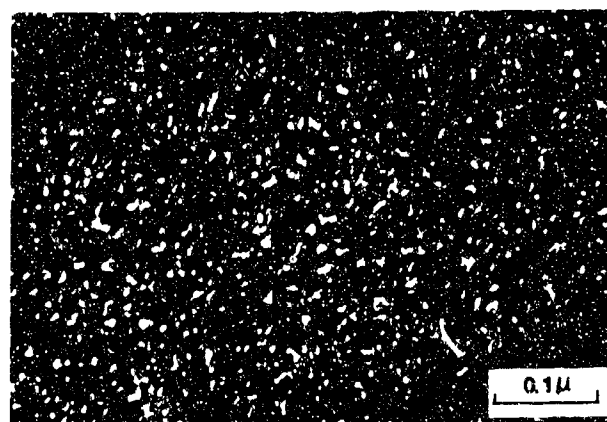
Thermal treatments that caused ordering in Ti-5Al-5Sn-5Zr also increased the susceptibility of Ti-5Al-2.5Sn (compare conditions 3F and 3E, Table II). However, no ordered domains or superlattice reflections were observed in this alloy using electron-microscopy techniques.

Fig. 6. Dark-field electron micrograph showing ordered domains of $Ti_3(Al, Sn)$ in Ti-5Al-5Sn-5Zr, condition 4L – (1650°F/1/2 hr/AC) + (1100°F/ 8 hr/FC) to (932°F/120 hr/AC), $[10\bar{1}1]\alpha_2$ reflection.
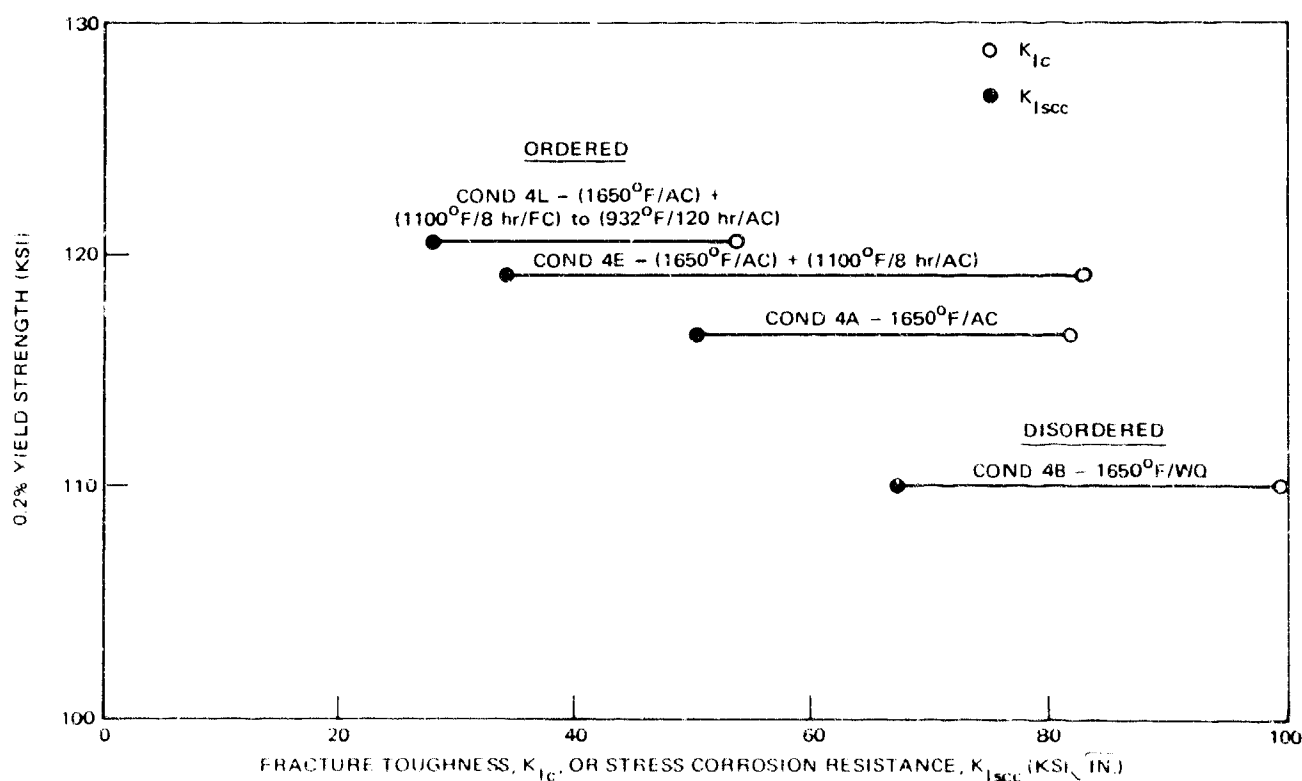

Fig. 7. Effect of order on the mechanical properties of Ti-5Al-5Sn-5Zr.

Apparently, the aluminum and tin levels are below the critical level required for order. The observed increase in susceptibility and the pronounced susceptibility in the solution-treated condition (condition 3F) are partially caused by transformation in the β phase. These transformations are discussed below.

The importance of slip mode on stress corrosion properties suggests that the residual dislocation structure also influences susceptibility. The dislocation structure was modified by varying the conditions of cold rolling and annealing to produce heavy cold work, recovery, and varying degrees of recrystallization. Figure 8 shows that 30-percent cold work increased the 0.2-percent yield strength of recrystallized Ti-5Al-5Sn-5Zr (condition 4A) without reducing the stress corrosion threshold. When compared in a more highly ordered condition (4E), the increased dislocation density improved both strength and K_{Iscc} (Figure 8). Although dislocation densities were not determined quantitatively, back-reflection Laue photographs (Figure 9) show that condition 4E was completely recrystallized, whereas condi-

tion 4KA retained evidence of heavy cold work. Changes in dislocation density have a similar affect on the susceptibility of α in Ti-70 and Ti-5Al-2.5Sn, although, in some cases, concurrent transformations in β have masked this trend (see Appendix A).

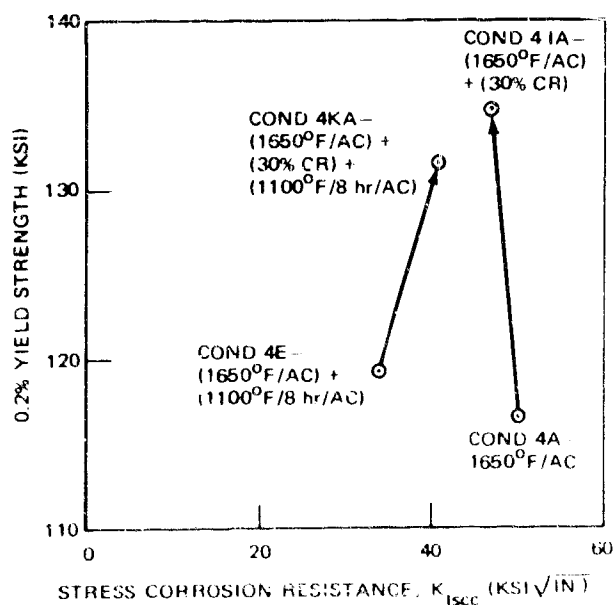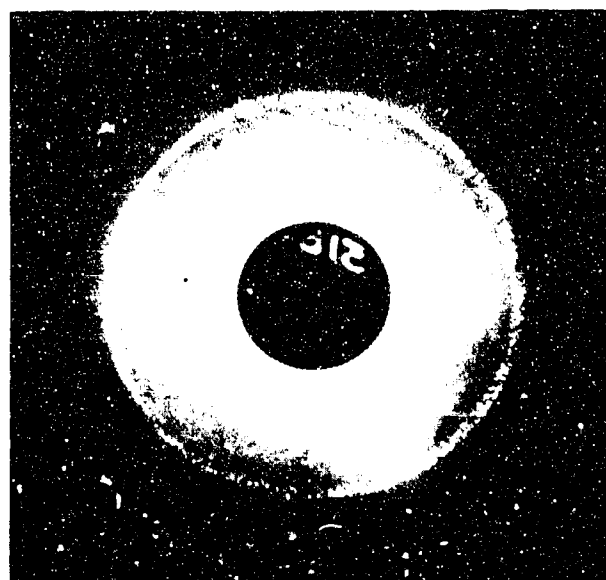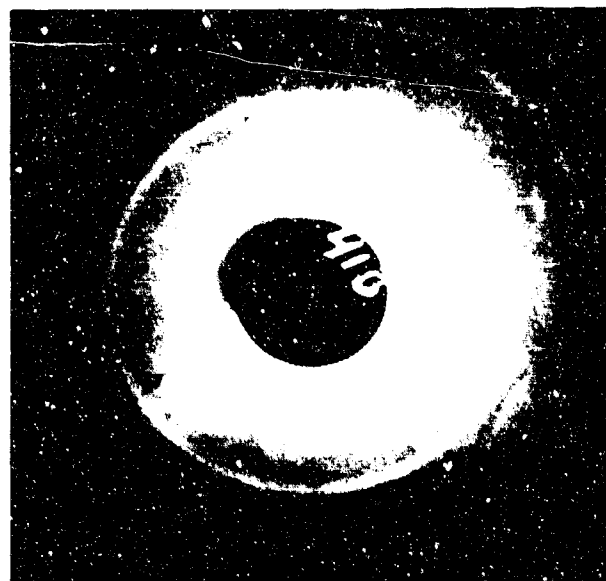(a)   Condition 4E $-$ (1650°F/1/2 hr/AC) + (1100°F/8 hr/AC)

Fig. 8.   Effect of cold work on the strength and stress-corrosion threshold of Ti 5Al-5Sn 5Zr

(b)   Condition 4KA $-$ (1650°F/1/2 hr/AC) + (30% CR) + (1100°F/8 hr/AC)

Fig. 9.   Back-reflection Laue photographs of Ti 5Al-5Sn-5Zr.

Grain Size and Morphology

Increasing the equiaxed α grain size of Ti-5Al-2.5Sn (Figure 10) reduced both stress corrosion resistance and the 0.2-percent yield strength. Table II shows K_{Iscc} decreased from 32 to 27 ksi $\sqrt{in}$. (conditions 3C and 3D). The reduction of 0.2-percent yield strength is qualitatively consistent with the analysis of Petch (15). Similar changes in grain size were achieved in Ti-70, but embrittling constituents in the β phase masked the expected grain-size dependence of SCC.
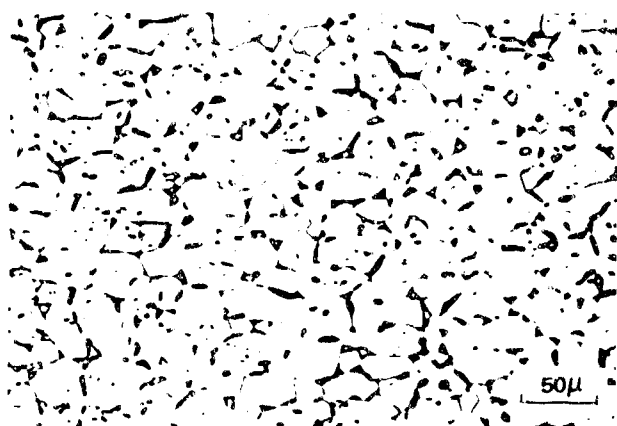
(a)   Condition 3C — 1650°F/10 hr/AC
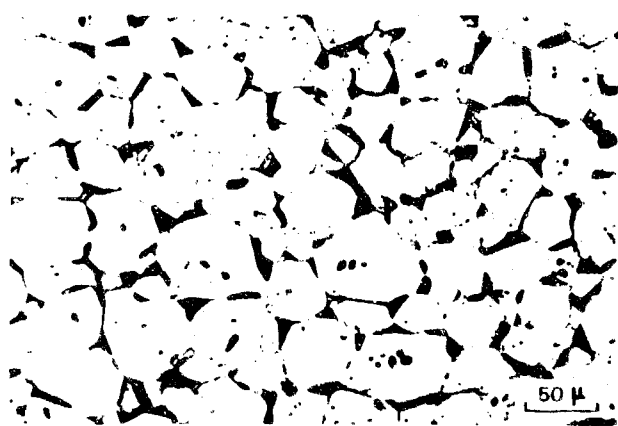
(b)   Condition 3D — 1650°F/100 hr/AC

Fig. 10. Primary α grain size in Ti-5Al-2.5Sn. Optical micrographs, Kroll's etch.

The grain size of Ti-70, Ti-5Al-2.5Sn, and Ti-5Al-5Sn-5Zr was reduced by transforming equiaxed α grains to an acicular morphology during solution treatment above the β transus. This treatment improves the stress corrosion resistance of $\alpha+\beta$ alloys. However, β-quenched Ti-5Al-5Sn-5Zr (condition 4D) is more susceptible to SCC than the α-quenched condition (4B) (Table II). Apparently, the martensite interface is not an effective barrier to slip in α alloys. Williams and Blackburn (16) have found unobstructed slip across several martensite plates in Ti-5Al-2.5Sn quenched from 2000°F. Under these conditions, the effective grain size is probably the large, prior β grain size. β-quenched Ti-70 (condition 2H, Table II) and Ti-5Al-2.5Sn (condition 3H) also show pronounced susceptibility but are more immune than the α-quenched conditions (2E and 3F, respectively). Susceptibility of the α-quenched conditions is related to ω formation in the β phase in the following section.

Transformations in β

Transformation of unstable β in Ti-70 and Ti-5Al-2.5Sn strongly influenced the mechanical properties of these alloys. In many cases, β transformations overshadowed structural changes in the α phase that were being related to SCC. Trace amounts of Fe (Table I) are responsible for the presence of β. X-ray analysis detected approximately 3 volume percent and 1.5 volume percent β in the mill-annealed condition of Ti-70 and Ti-5Al-2.5Sn, respectively.

Thin-foil studies showed unstable β precipitated ω and/or α, depending on the conditions of heat treatment. Extremely fine ω (< 25Å diameter) was formed in Ti-70 during air cooling from 1200°F and 1300°F. The particles were too small for direct imaging with the electron microscope and were detected from diffuse spots in the electron diffraction patterns. Diffuse ω was also detected in the β phase of all conditions of Ti-5Al-2.5Sn except 3F, 3H, and 3JA (Appendix A). Its presence in α-quenched Ti-5Al-2.5Sn (condition 3F, Table

II) reduced K_{Iscc} below the level for the β-quenched condition (3H), even though the effective grain size was larger for the β-quenched condition.

Higher solution temperature reduced the Fe content of β and allowed more extensive transformation during cooling. In Ti-70, approximately 50 volume percent ω (100 Å diameter) was formed in β during cooling from 1500°F (Figure 11). This additional ω reduced stress corrosion resistance to that shown in Figure 12. Solution treatment at 1700°F (condition 2H, Table II) transformed β to martensite and improved K_{Iscc} to the highest level measured for this alloy.

Isothermal aging at temperatures above the maximum temperature of ω stability (approximately 700°F) decomposed ω and precipitated α in β by a cellular mechanism. Transforming ω present in the 1500°F water-quenched condition of Ti-70 (Figure 11) to α by annealing at 1050°F for 30 minutes improved K_{Iscc} from 34 to 39 ksi $\sqrt{in}$. (conditions 2E and 2F, Table II). However, further annealing at 1050°F for 20 hours (condition 2G) reduced K_{Iscc} to the level measured for the 1500°F water-quenched condition. This behavior suggests that a large volume fraction of α can embrittle β as effectively as ω, which
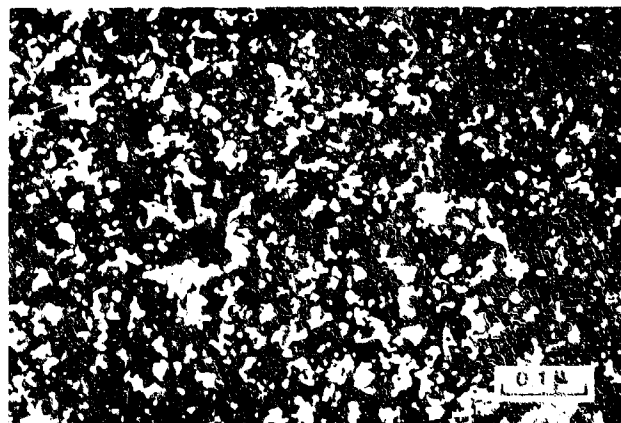
Fig. 11. Dark-field electron micrograph of ω in β of Ti-70, condition 2E—1500°F/1/2 hr/WQ, (1011) ω reflection.
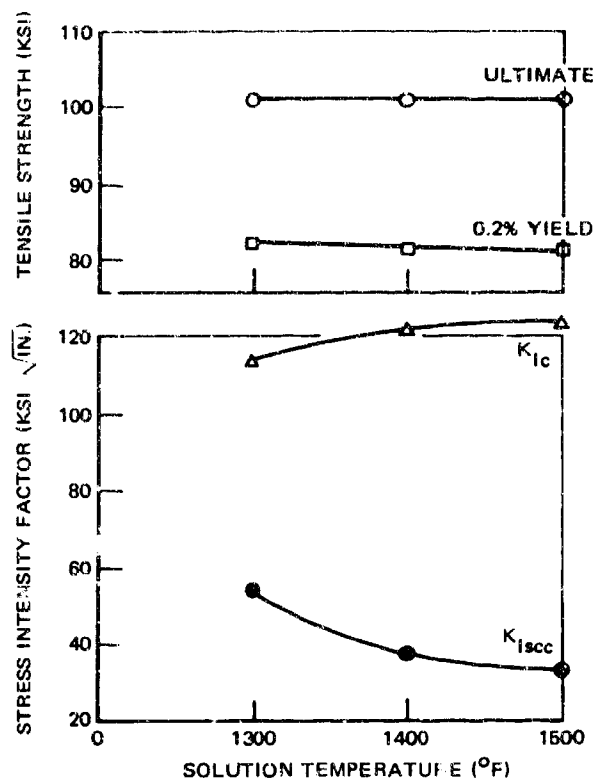
Fig. 12. Effect of solution temperature on the properties of Ti-70—solution-treated 1/2 hr and air cooled.

is consistent with the results of Harmon and Troiano (17). In Ti-5Al-2.5Sn, transformation of diffuse ω to α reduced K_{Iscc} from 26 ksi $\sqrt{in}$. (condition 3A, Table II) to 21 ksi $\sqrt{in}$. (condition 3E). Electron micrographs of β containing diffuse ω and α are presented in Figure 13. Coplanar dislocation arrays characteristic of Ti-5Al-2.5Sn are visible in Figure 13(a).

α + β Alloys

Mechanical-property tests (see Appendix B) have been conducted on 11 α+β alloys: Ti-2.25Al-11Sn-4Mo-0.2Si (IMI 680), Ti-4Al-3Mo-1V, Ti-4Al-4Mo-2Sn-0.5Si (Hylite 50), Ti-5Al-3Mo-1V-2Sn, Ti-6Al-4V, Ti-6Al-2Mo, Ti-6Al-6V-2Sn, Ti-6Al-5Zr-1V-0.25i (IMI 684), Ti-7Al-2.5Mo, Ti-7Al-4Mo, and Ti-8Al-1Mo-1V. Mill-annealed properties are compared
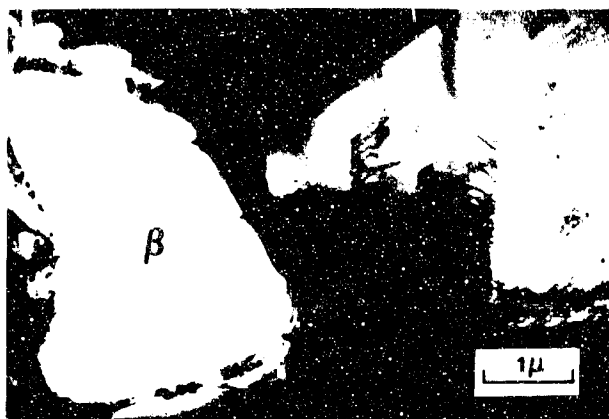
(a) Containing unresolved diffuse ω, condition 3A—1400°F/2 hr/AC.

(b) Containing α, condition 3E—(1400°F/2 hr/AC) + (1100°F/8 hr/FC) to (932°F/120 hr/AC).

(c) Dark field micrograph of condition 3E showing the Widmanstatten morphology of α in β.

Fig. 13. Electron micrographs of β in Ti-5Al-2.5Sn.

with those of the α alloys in Figure 14. This figure shows that the addition of β stabilizing elements increased alloy strength and often improved stress corrosion resistance. Stress corrosion resistance improved with increased volume percent β stabilized by isomorphous-type β stabilizers (Mo and/or V) (Figure 15). Similar β-STA heat-treatment conditions were selected for each alloy included in Figure 15, e.g. β anneal, solution treat (β transus temperature -75°F, water quench), and age (1100°F to 1250°F, 4 hours, air cool).

In addition to the effect of volume percent β on stress corrosion resistance, Figure 15 shows that aluminum content above approximately 6 weight percent promotes susceptibility. In alloys with greater than 6 weight percent aluminum, increasing the degree of order further increased susceptibility. In Ti-7Al-2.5Mo, K_{Iscc} decreased from 80 ksi $\sqrt{in.}$ (condition 27B, Table III), to 65 ksi $\sqrt{in.}$ (27D), to 44 ksi $\sqrt{in.}$ (27E) as the degree of order increased.

Although β stabilized by isomorphous elements improves stress corrosion resistance, tests on Ti-6Al-6V-2Sn and Ti-4Al-4Mo-2Sn-0.5Si (Hylite 50) suggest that β eutectoid stabilizers (Fe and/or Cu and Si) promote susceptibility. Ti-6Al-6V-2Sn containing 0.7 weight percent Fe and 0.7 weight percent Cu is more susceptible (K_{Iscc}/K_{Ic} = 0.63) than similar alloys containing only isomorphous stabilizers (Figure 15). In addition, Ti-4Al-4Mo-2Sn-0.5Si exhibits greater susceptibility (K_{Iscc}/K_{Ic} = 0.50) than two similar alloys (Ti-4Al-3Mo-1V and Ti-5Al-3Mo-1V-2Sn) that do not contain silicon (Figure 15).

The intermetallic phase (Ti_2Cu or Ti_5Si_3) should be present in most heat-treat conditions of these alloys, because the eutectoid reaction ($\beta \rightarrow \alpha + TiX$) is "extremely active" in the Ti-Cu and Ti-Si systems (18). In Ti-Cu binary alloys containing 2, 4, 6, and 8 weight percent Cu, Ti_2Cu has been observed in both quenched and quenched and aged conditions (19). Efforts to

11
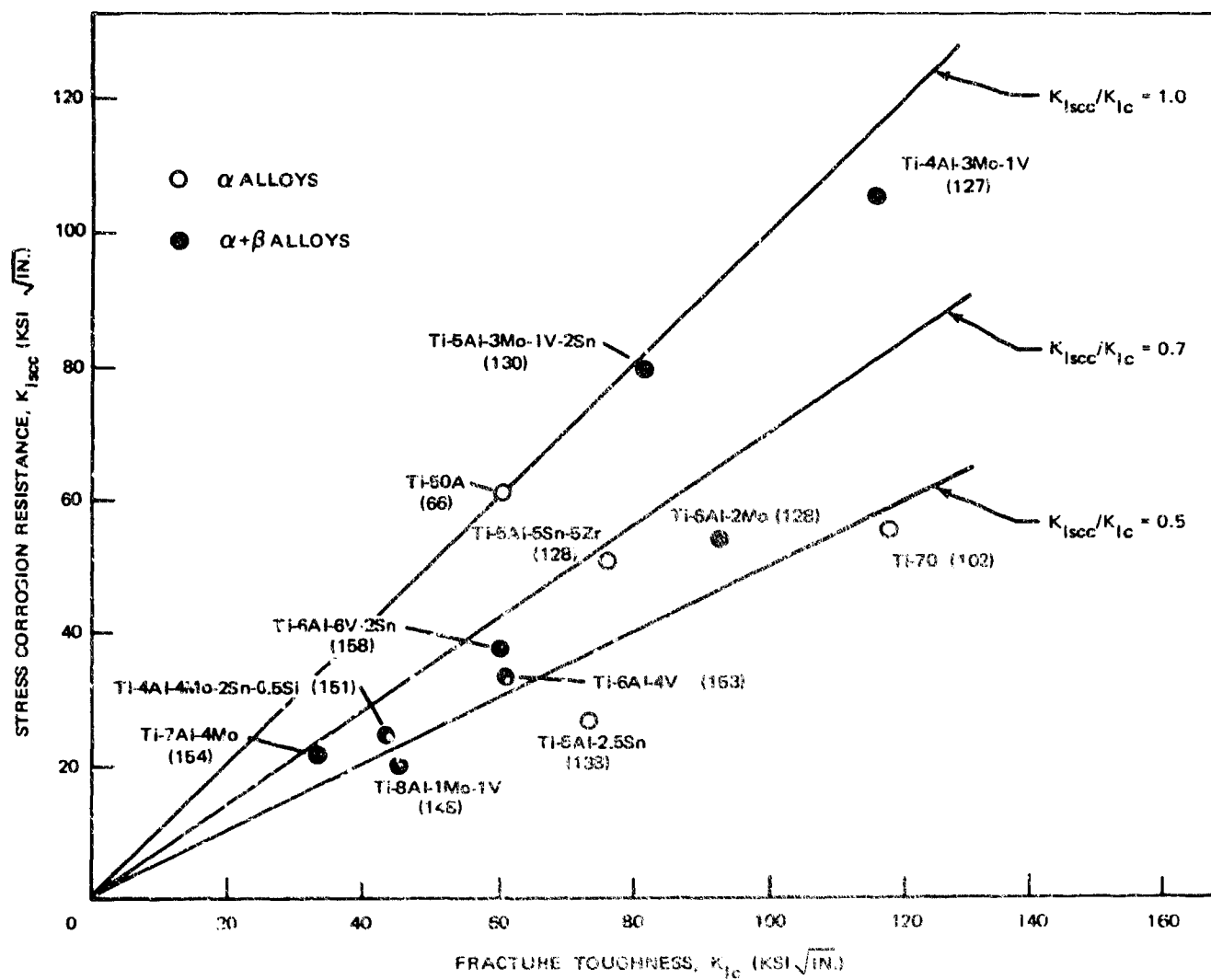
Fig. 14. Mill-annealed properties of α and α+β titanium alloys; ultimate tensile strength in ksi is shown in parenthesis.
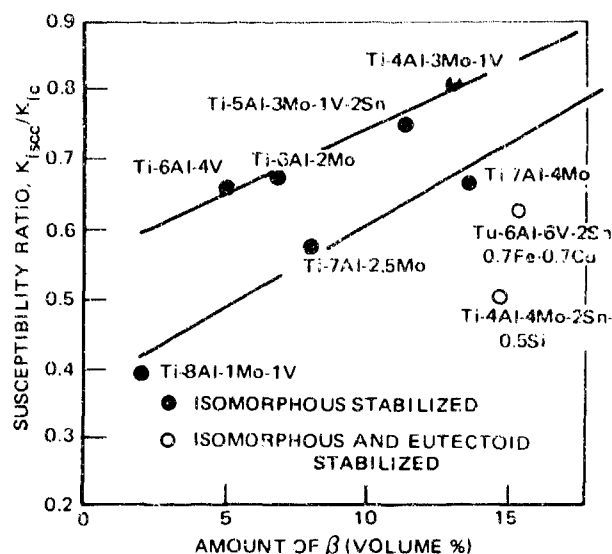
Fig. 15. Effect of β on stress-corrosion susceptibility
of titanium alloys in a β-STA heat-treatment
condition.

identify this phase in Ti-6Al-6V-2Sn have been unsuccessful, either because of the low Cu content or the complex morphology of transformed β. In quenched Ti-4Al-4Mo-2Sn-0.5Si, particles were observed in both transformed β (Figure 16) and primary α (Figure 17). Particles in the primary α phase were sufficiently large for identification as Ti_5Si_3 by electron diffraction. Based on the work of Antony et al. (20) on the Ti-Al-Si system, the silicide compound in this alloy should be stable up to approximately 1780°F.

Ti-4Al-4Mo-2Sn-0.5Si was heat treated and thermomechanically processed in an attempt to reduce the embrittlement characteristic of alloying with β eutectoid stabilizers. Increased aging temperature from 932°F to 1300°F

Table III. Strength and fracture properties of Ti-7Al-2.5Mo
in selected conditions.

Identification	Condition	UTS (ksi)	0.2% yield (ksi)	K_{Ic} (ksi $\sqrt{in.}$)	K_{Iscc} (ksi $\sqrt{in.}$)
27A	50% HR (1750°F)	147.5	135.5	65	45
27B	1675°F/1/2 hr/WQ	137.8	106.0	95	80
27D	1650°F/1/2 hr/AC	139.6	127.1	96	65
27E	(1650°F/1/2 hr/FC) to (932°F/120 hr/AC)	135.9	122.6	74	44
27F	(1800°F/1/2 hr/WQ) + (1100°F/8 hr/AC)	166.6	151.9	52	37
27H	(1900°F/1/2 hr/AC) + (1800°F/1/2 hr/WQ) + (1100°F/8 hr/AC)	158.4	134.8	72	43
27K	(50% HR) + (30% CR)	160.9	143.1	83	61

HR = hot rolled   WQ = water quenched
CR = cold rolled   AC = air cooled

(a) Bright field.
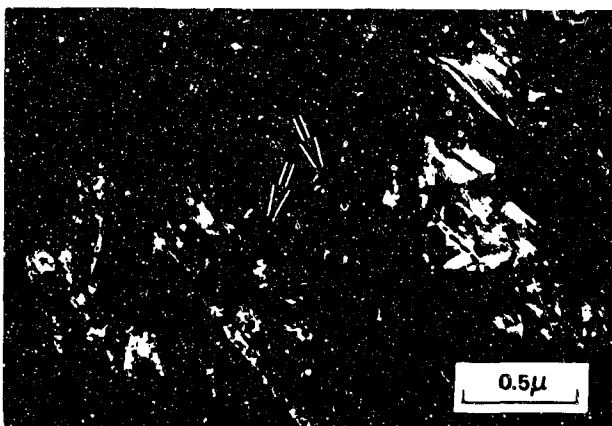
(b) Dark field.

Fig. 16. Electron micrographs of particles tentatively identified as Ti_5Si_3 in the transformed β region of Ti-4Al-4Mo-2Sn-0.5Si (Hylite 50), condition 13A—1650°F/1/2 hr/WQ.
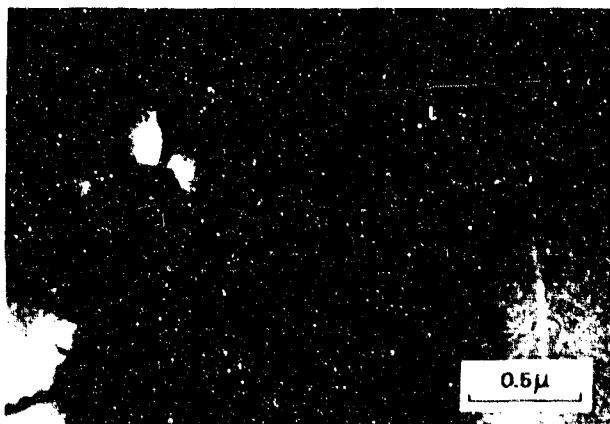
Fig. 17. Ti_5Si_3 particles in the primary α phase of Ti-4Al-4Mo-2Sn-0.5Si (Hylite 50), condition 13A—1650°F/1/2 hr/WQ.

coarsened the transformed structure (Figure 18) and reduced strength as expected but also reduced K_{Ic} and K_{Iscc} (Figure 19). However 20-percent rolling prior to aging at 932°F (conditions 13JA and 13JB) increased the 0.2-percent yield strength by 20 ksi without significantly changing K_{Ic} or K_{Iscc} (Figure 20). Both thermomechanical treatments increased dislocation density and nucleated additional α and Ti_5Si_3 in the β phase. Additional nucleation by "duplex aging" (condition 13K) also
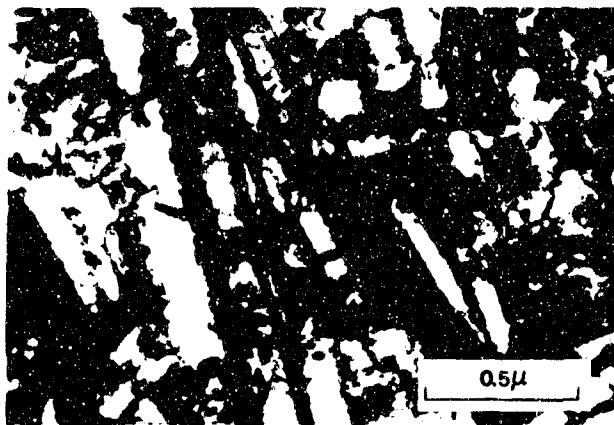
(a) Condition 13C — (1650°F/1/2 hr/AC) + (932°F/24 hr/AC)
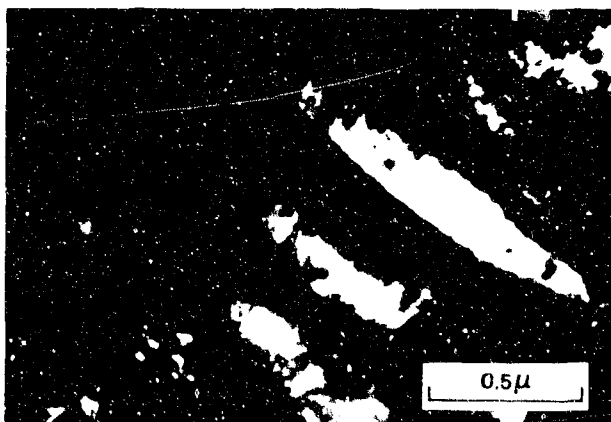
(b) Condition 13E — (1650°F/1/2 hr/AC) + (1300°F/24 hr/AC)

Fig. 18. Effect of aging temperature on transformed β in Ti-4Al-4Mo-2Sn-0.5Si (Hylite 50).

14
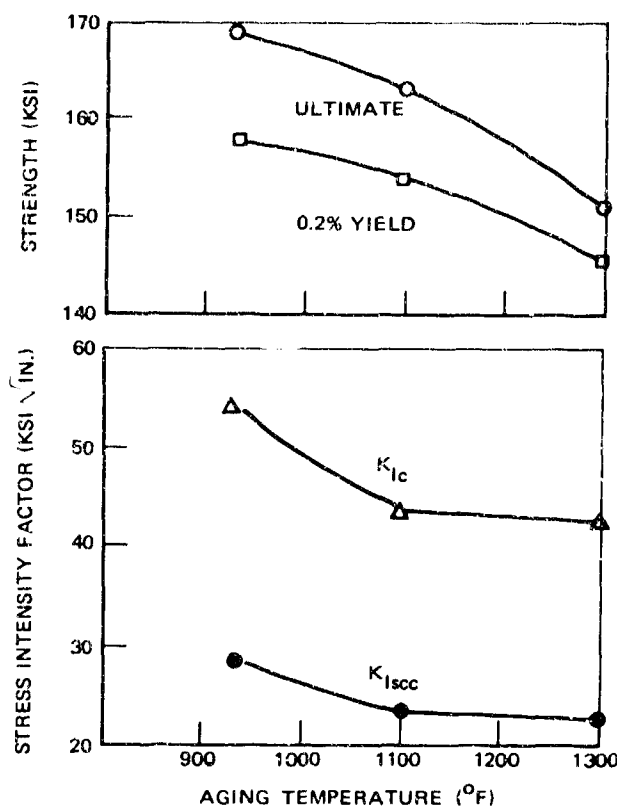
Fig. 19 Effect of aging temperature on the properties of Ti-4Al-4Mo-2Sn-0.5Si (Hylite 50)—solution treated (1650°F/1/2 hr/AC) before aging at temperature shown for 24 hrs and air cooled.

improved mechanical properties. The changes were small for strength and stress corrosion resistance but fracture toughness improved markedly (Figure 20). In Ti-7Al-2.5Mo, defor: ion increased strength, toughness, and stress rrosion resistance (compare 27A and 27K, Table III). Rolling Ti-4Al-4Mo-2Sn-0.5Si prior to solution treatment (condition 13L) reduced the primary α grain size by recrystallization. This refine.nent raised K_{Ic} from 55 to 72 ksi $\sqrt{in}$. and K_{Iscc} from 27 to 36 ksi $\sqrt{in}$. without affecting the strength (Figure 20).

Refining primary α by transforming equiaxed grains to an acicular morphology improved the fracture properties of both Ti-4Al-4Mo-2Sn-0.5Si (conditions 13C and 13I, Figure 20)

and Ti-7Al-2.5Mo (compare 27F and 27H, Table III). This is consistent with the behavior of other $\alpha + \beta$ alloys, including Ti-6Al-4V and Ti-4Al-3Mo-1V (5), Ti-6Al-6V-2Sn and Ti-7Al-4Mo (21), and Ti-6Al-2Mo and Ti-5Al-3Mo-1V-2Sn (22).

DISCUSSION

Stress corrosion resistance was found to be microstructure dependent for a wide range of titanium alloy compositions and thermo-mechanical conditions. Alloys that exhibited coplanar slip in the α phase also showed pronounced susceptibility to SCC. Coplanar slip is characteristic of alloys containing (1) high oxygen (3800 ppm, Ti-70), (2) aluminum in excess of approximately 6 weight percent (e.g. Ti-6Al-4V, Ti-7Al-2.5Mo, and Ti-8Al-1Mo-1V), or (3) 5 weight percent or greater aluminum and 2.5 weight percent or greater tin (Ti-5Al-2.5Sn and Ti-5Al-5Sn-5Zr).

Restricting slip in this manner is thought to promote stress corrosion susceptibility by intensifying the dislocation pileup stress. This stress represents a large component normal to the fracture plane of grains unfavorably oriented for slip (23). Intensification of the normal stress to a critical value initiates trans-granular cleavage cracks of the type observed in the α phase of susceptible alloys (Figure 4). Other α grains having a high resolved shear stress for slip exhibit ductile tearing (Figure 4). In immune alloys, such as Ti-50A. the fracture stress is not reached for any grain orientation because cross slip limits the magnitude of the stress concentration.

Formation of ordered domains of Ti_3Al or $Ti_3(Al,Sn)$ in the α phase further restricted slip and increased stress corrosion susceptibility. Speidel (24) has shown that precipitation of coherent particles (e.g. ordered domains) promotes planar slip. Ti-5Al-5Sn-5Zr containing ordered domains appeared to have a reduced slipband thickness compared to the disordered condition (Figure 5). The decreased slipband thickness is thought to increase

15
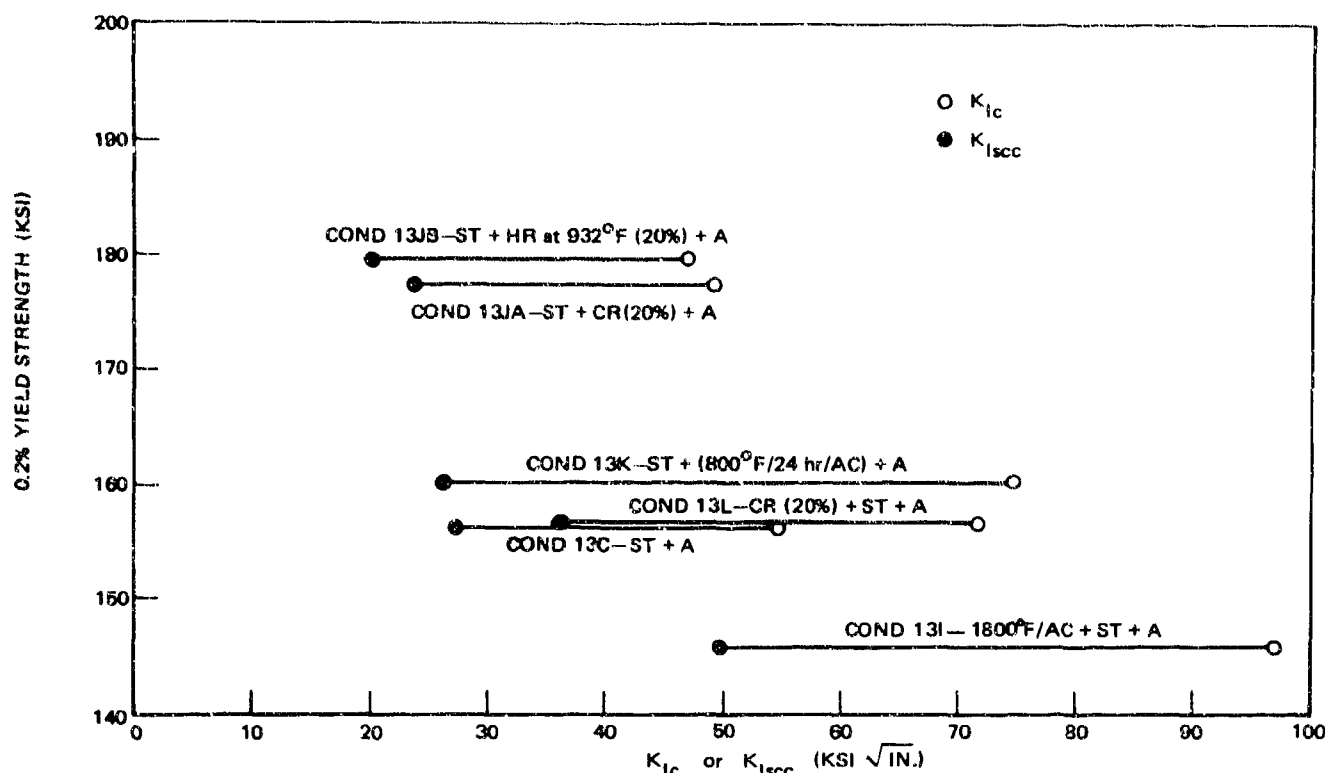
Fig. 20. *Properties of Ti-4Al-4Mo-2Sn-0.5Si (Hylite 50) in several heat-treated and thermomechanically processed conditions; ST = 1650°F/1/2 hr/AC, A = 932°F/24 hr/AC.*

susceptibility by reducing the probability of activating a dislocation source across a grain boundary and intensifying the dislocation pileup stress (25).

In alloys that exhibit coplanar slip, increasing the slip length intensifies the stress at the head of a dislocation pileup (26). This is thought to be the reason that stress corrosion susceptibility increased with grain size in Ti-5Al-2.5Sn (Figure 10). Other α and $\alpha + \beta$ alloys that slip in a coplanar manner should show a similar grain-size dependence, because the effective slip length is the equiaxed α grain size in recrystallized material. Reducing the α grain size of Ti-4Al-4Mo-2Sn-0.5Si by recrystallization (condition 13L) improved both fracture toughness and stress corrosion resistance (compare 13L and 13C, Figure 20). In cold-worked material, the effective slip length may be reduced by increased dislocation density. This would account for the improved pro-

perties observed in cold-worked Ti-5Al-5Sn-5Zr (Figure 8), Ti-7Al-2.5Mo (compare 27A and 27K, Table III), and Ti-4Al-4Mo-2Sn-0.5Si (compare 13C and 13JA, Figure 20).

Stress corrosion resistance improved with increased volume percent β stabilized by isomorphous-type elements Mo and/or V (Figure 15). This is attributed to the ability of β (ductile) to arrest stress corrosion cracks that propagate readily through the α phase (5, 12, 27). However, precipitation of a second phase in β can markedly reduce stress corrosion resistance. Extremely fine ω in the β phase of Ti-70 is thought to be responsible for reducing K_{Iscc} from 70 ksi $\sqrt{in}$. (condition 2H, no ω) to 54 ksi $\sqrt{in}$. (condition 2A, $\omega < 25$ Å diameter). Larger ω particles (approximately 100 Å diameter, Figure 11) further reduced stress corrosion resistance; K_{Iscc} changed from 54 ksi $\sqrt{in}$. to 33 ksi $\sqrt{in}$. (Figure 12). A large volume fraction of α in β resulted in an equally

16

low threshold (condition 2G, Table II). In Ti-5Al-2.5Sn stress corrosion resistance was also dependent on the condition of the β phase. In alloys containing Cu or Si, low-stress-corrosion properties (Figure 15) are attributed to precipitation of α and intermetallic compounds Ti_2Cu or Ti_5Si_3 in β. These intermetallics, as well as ω and α, are thought to enhance susceptibility by nucleating cracks in the β phase. Holden et al. (28) have attributed pronounced tensile embrittlement of a β titanium alloy to a fine dispersion of ω.

Ti-4Al-4Mo-2Sn-0.5Si was thermomechanically processed in an attempt to improve mechanical properties by controlling the transformed β morphology, including Ti_5Si_3 particle size. Overaging to coarsen the transformed structure (Figure 18) reduced strength as expected, but it also lowered fracture toughness and stress corrosion resistance (Figure 19). Overaging a similar alloy that did not contain Si (Ti-4Al-3Mo-1V) caused similar structure and property changes, except the fracture properties increased markedly (5). The reduced fracture properties of Ti-4Al-4Mo-2Sn-0.5Si are thought to result from an increase in Ti_5Si_3 particle size. However, it was not possible to positively relate Ti_5Si_3 particle size to mechanical properties because of the complex morphology of the transformed region (Figure 18). Refining the transformed structure by "duplex aging" (condition 13K) to nucleate additional α and Ti_5Si_3 in β improved the combination of strength and stress corrosion resistance (compare conditions 13C and 13K, Figure 20). Refining the transformed structure by deformation to provide additional heterogeneous nucleation sites for β decomposition also improved mechanical properties (compare conditions 13C, 13JA, and 13JB Figure 20). Both reduced particle size and increased dislocation density are thought to contribute to the improved properties of conditions 13JA and 13JB.

CONCLUSIONS

1. The loading sequence for stress corrosion testing has a varied, often pronounced effect on the stress corrosion threshold K_{Iscc}. Loading in salt solution reduced the threshold of certain alloy heat-treatment conditions as much as 65 percent compared to loading in air before adding salt solution. However, conditions that are either markedly susceptible or nearly immune to SCC are unaffected by the loading sequence. Conclusions 2 through 5 are based on thresholds established from salt-loaded specimens.

2. Alpha titanium containing approximately 1200 ppm oxygen (Ti-50A) is immune to SCC. Increasing oxygen to 3800 ppm (Ti-70) or adding aluminum (e.g. Ti-6Al-4V, Ti-7Al-2.5Mo and Ti-8Al-1Mo-1V) or aluminum and tin (Ti-5Al-2.5Sn and Ti-5Al-5Sn-5Zr) restricts slip in the α phase and promotes stress corrosion susceptibility. Restricted slip is thought to promote stress corrosion through its effect on the dislocation pileup stress. Formation of ordered domains of $Ti_3(Al,Sn)$ in Ti-5Al-5Sn-5Zr reduced the thickness of $\{10\bar{1}0\}$ slipbands and further lowered K_{Iscc}.

3. Stress corrosion resistance increases with decreasing slip length in alloys that exhibit coplanar slip. The effective slip length is the α grain size in α and $\alpha+\beta$ alloys and the prior β grain size in water-quenched α alloys. Increasing the dislocation density by cold work reduced the effective slip length and improves stress corrosion resistance.

4. Strength and relative stress corrosion resistance improve with increased volume percent β stabilized by isomorphous-type stabilizers Mo and/or V. Precipitation of a second phase in β, however, can markedly reduce the stress corrosion threshold. ω, α, and intermetallic compounds all cause pronounced embrittlement when present as

17

particles with a diameter of the order of 100 Å. Intermetallic compounds are observed in alloys containing silicon and copper.

5. Combining plastic deformation with solution treating and aging improves the combination of strength, toughness, and stress corrosion resistance of Ti-4Al–4Mo- -2Sn-0.5Si. Deformation after solution treatment but prior to aging provided additional heterogeneous nucleation sites for β decomposition and refined the transformed structure. Deformation prior to solution treatment and aging recrystallized primary α and reduced α grain size.

ACKNOWLEDGEMENT

REFERENCES

1. R. E. Curtis, S. H. Smith, and W. F. Spurr, Titanium Alloy Selection Report, Boeing Document D6-19729, September 30, 1965.

2. R. W. Judy and R. J. Goode, Stress-Corrosion Cracking of Titanium Alloys in Salt Water, NRL Report No. 6564, July 21, 1967.

3. I. R. Lane and J. L. Cavallaro, Metallurgical and Mechanical Aspects of Sea-Water Stress Corrosion of Titanium, Applications Related Phenomena in Titanium Alloys, ASTM STP 432, ASTM (1968) 147.

4. Titanium Development Program, Boeing Document D6A10065-1, March 28, 1966.

5. R. E. Curtis and W. F. Spurr, Effect of Microstructure on the Fracture Properties of Titanium Alloys in Air and Salt Solution, ASM Trans. Quart., 61 (March 1968) 115.

6. D. E. Piper, S. H. Smith, and R. V. Carter, Corrosion Fatigue and Stress Corrosion Cracking in Aqueous Environments, Metals Engr. Quart., 8 (Aug 1968) 50.

7. B. F. Brown, A New Stress Corrosion Cracking Test for High Strength Alloys, Materials Research Standards, 6 (March 1966) 129.

8. W. F. Brown, Jr., and J. E. Srawley, Plane Strain Crack Toughness Testing of High Strength Metallic Materials, ASTM STP 410, ASTM (1966).

9. M. J. Blackburn and J. C. Williams, The Preparation of Thin Foils of Titanium Alloys, AIME Trans., 239 (February 1967) 287.

10. M. F. Schurmann and W. C. Larson, Test of Ti-6Al-4V Post Exposure Specimens for Corrosion Susceptibility Using Defined Techniques, Group Report T6A10957-2TN, Report No. 12, July 17, 1968.

11. ARPA Coupling Program on Stress-Corrosion Cracking (Second Quarterly Report), NRL Memorandum Report 1775, April 1967.

12. D. N. Fager and W. F. Spurr, Some Characteristics of Aqueous Stress Corrosion in Titanium Alloys, ASM Trans. Quart., 61 (June 1968) 283.

13. S. R. Seagle, The Influence of Microstructure and Composition on the Properties of Alpha-Beta Titanium, Titanium Metallurgy Course, New York University, September 13, 1965.

14. A. T. Churchman, The Slip Modes of Titanium and the Effect of Purity on Their Occurrence During Tensile Deformation of Single Crystals, Proc. Roy. Soc., A226 (1954) 216.

15. N. J. Petch, Cleavage Strength of Polycrystals, J Iron Steel Inst., 173 (1954) 25.

16. M. J. Blackburn and J. C. Williams, Metallurgical Aspects of Stress Corrosion Cracking, presented at Fundamental Aspects of Stress Corrosion Cracking, Columbus, Ohio, September 1967.

17. B. L. Harmon and A. R. Troiano, Beta Transformation Characteristics of Titanium Alloyed with Vanadium and Aluminum, Trans. ASM, 53 (1961) 43.

18. R. I. Jaffee, The Physical Metallurgy of Titanium Alloys, Progress in Metal Physics, Vol. 7, Pergamon Press, 1958, p. 65.

19. J. C. Williams, D. H. Polonis, and R. Taggart, An Electron Microscopy Study of Ti-Cu Alloys, presented at Winter Meeting of AIME, New York, 1968.

20. K. C. Antony and J. W. Clark, Dispersion Strengthened Alpha Titanium Alloys, Technical Report AFML TR 66-105, May 1966.

21. P. T. Finden, Comparison of Titanium Alloys 6Al-6V-2Sn and 7Al-4Mo, Boeing Engineering Report No. 6-7620-13-PMR3, February 16, 1967.

22. P. T. Finden, Evaluation of Ti-6Al-2Mo and Ti-5Al-3Mo-1V-2Sn, Boeing Document D6-19765, March 13, 1967.

23. A. N. Stroh, A Theory of Fracture in Metals, Advances in Physics, 6 (1957) 418.

24. M. O. Speidel, Coherent Particles and Stress Corrosion Cracking of High Strength Aluminum Alloys, Proceedings of the Air Force Materials Laboratory Fiftieth Anniversary Technical Conference on Corrosion of Military and Aerospace Equipment, Tech. Report AFML-TR-67-329 (Nov. 1967) p. 1915.

25. A. J. McEvily, Jr., and T. L. Johnston, The Role of Cross-Slip in Brittle Fracture and Fatigue. Proc. of First International Conference on Fracture, Japanese Society for Strength and Fracture of Materials, Japan (1966) 515.

26. A. H. Cottrell, Theory of Brittle Fracture in Steel and Similar Metals, AIME Trans., 212 (1958) 192.

27. J. C. Williams, R. R. Boyer, and M. J. Blackburn, The Influence of Microstructure on the Fracture Topography of Titanium Alloys, Boeing Document D6-23622, June 1968.

28. F. C. Holden, H. R. Ogden, and R. I. Jaffee, J. Metals (May 1956) 521.

29. P. T. Finden, Environmental Crack Growth Susceptibility of Titanium EX 684, Boeing Engineering Report No. 6-7620-13-PMR2, February 2, 1967.

Strength, Toughness, and Stress Corrosion Properties
of α Titanium Alloys

Alloy & identification	Condition	UTS (ksi)	0.2% yield (ksi)	% elong (in 1 in.)	R.A. (%)	E (ksi x 10^{-3})	$P_{5\%}$* (kips)	P_{max} (kips)	Notch bend thickness (in.)	K_{Ic} (ksi $\sqrt{in.}$)	K_{Iscc}** (ksi $\sqrt{in.}$)
Ti-50A											
1A	1300°F/1/2 hr/AC	65.8	42.5	34.0	66		25.8	43.50	1.0	60	60
Ti-70											
2A	1300°F/1/2 hr/AC	102.2	84.3	24.0	66.5	16.7	24.88	26.93	0.48	114	54 (86)
2B	1400°F/1/2 hr/AC	101.3	83.6	24.5	67.5	16.9	26.13	26.63	0.48	121	38 (84)
2C	1500°F/1/2 hr/AC	102.0	83.2	25.5	67.5	16.9	27.1	28.58	0.48	123	33 (92)
2D	1500°F/20 hr/AC	99.7	79.6	24.0	63.0	16.5	24.08	24.08	0.48	111	33 (33)
2E	1500°F/1/2 hr/WQ	106.5	84.6	22.0	62.0	17.0	27.33	29.05	0.48	128	34 (34)
2F	(1500°F/1/2 hr/WQ) + (1050°F/1/2 hr/AC)	103.2	82.5	25.0	68.0	17.0	23.60	24.70	0.48	113	39 (75)
2G	(1500°F/1/2 hr/WQ) + (1050°F/20 hr/AC)	101.1	82.2	25.5	67.0	16.6	25.05	27.05	0.48	113	33 (89)
2H	1700°F/1/2 hr/WQ	100.9	76.5	23.0	55.0	16.4	19.88	20.18	0.48	105	70 (90)
2I	(1700°F/1/2 hr/WQ) + (1050°F/1/2 hr/AC)	101.8	77.2	22.5	51.5	16.7	19.93	20.05	0.48	96	48 (82)
2JA	30% CR	129.2	115.2	18.0	70.5	15.5	10.78	10.78	0.30	82	33 (46)
2JB	(30% CR) + (925°F/1/2 hr/AC)	111.4	98.6	23.0	72.5	16.1	14.70	15.70	0.30	116	50
2K	(30% CR) + (1200°F/1/2 hr/AC)	103.7	88.0	28.0	69.5	15.1	11.75	17.2	0.30	92	55
2L	(30% CR) + (1500°F/1/2 hr/AC)	102.4	85.5	30.0	66.7	15.3	11.63	15.90	0.30	91	38
2M	60% CR	136.5	121.4	16.0	71.0	14.6	3.67	3.67	0.20	45	40
2N	30% HR at 1100°F	108.-	94.4	24.0	75.5	15.7	14.02	14.16	0.30	115	34
2O	30% HR at 1500°F	107.1	87.6	28.0	68.5	15.7	12.49	15.90	0.30	104	35
2P	30% HR at 1700°F	111.8	86.9	29.3	56.0	16.8	11.46	11.46	0.30	93	54

21

Alloy & identification	Condition	UTS (ksi)	0.2% yield (ksi)	% elong (in 1 in.)	R.A. (%)	E (ksi x 10^3)	$P_{5\%}$ (kips)	P_{max} (kips)	Notch bend thickness (in.)	K_{Ic} (ksi $\sqrt{in.}$)	K_{Iscc}** (ksi $\sqrt{in.}$)
Ti-5Al-2.5Sn											
3A	1400°F/2 hr/AC	138.2	129.2	19	42	19.0	15.26	15.36	0.48	72	26
3B	1650°F/1 hr/AC	134.2	126.5	19	48	19.6	19.00	19.05	0.48	88	30
3C	1650°F/10 hr/AC	132.1	125.1	18.5	48	20.4	18.86	18.86	0.48	90	32
3D	1650°F/100 hr/AC (in argon)	130.3	118.7	19.0	41.5	18.5	19.68	19.68	0.48	92	27
3E	(As recvd) + (1100°F/ 8 hr/FC) to (2°F/ 120 hr)	139.8	130.5	14.5	22.5	18.5	9.44	9.44	0.48	46	21
3F	1650°F/1 hr/WQ	135.4	124.2	17.5	46.5	18.3	22.16	22.16	0.48	103	27
3G	1850°F/1 hr/WQ	40.1	127.8	17.5	45.5	22.0	23.38	25.33	0.48	116	31
3H	2000°F/1/2 hr/WQ	140.0	126.6	14.0	28.5	16.8	24.68	26.71	0.48	119	37
3I	(1850°F/1 hr/WQ) + (1250°F/8 hr/AC)	139.4	129.3	19.0	43.5	18.3	17.59	17.59	0.48	83	23
3JA	(30% CR) + (1100°F/8 hr/FC) to (932°F/120 hr/AC)	158.0	145.4	14.0	42.5	---	6.33	6.33	0.30	43	19
3KA	(30% CR) + (1400°F/1 hr/AC)	140.9	129.1	15.0	47.5	---	11.98	11.98	0.30	86	36
3KB	(30% CR) + (1650°F/1 hr/AC)	136.6	124.5	20.0	50.5	---	15.1	16.4	0.30	115	24
3LA	30% CR	166.2	151.2	12.0	42.5	---	8.95	8.95	0.30	60	38
Ti-5Al-5Sn-5Zr											
4A	1650°F/1/2 hr/AC	128.2	116.5	17.0	38.5	17.2	17.45	17.87	0.48	83	50
4B	1650°F/1/2 hr/WQ	126.9	109.7	17.5	38.5	17.0	21.35	22.05	0.48	101	67
4C	1750°F/1/2 hr/WQ	128.5	109.9	16.0	39.5	16.9	27.04	28.03	0.48	131	81
4D	1850°F/1/2 hr/WQ	136.6	114.1	15.5	36.5	17.2	19.58	20.43	0.48	102	55
4E	(1650°F/1/2 hr/AC) + (1100°F/8 hr/AC)	126.0	119.2	17.5	37.5	17.5	17.48	17.53	0.48	83	44
4F	(1750°F/1/2 hr/WQ) + (1250°F/8 hr/AC)	127.9	116.7	17.0	34.5	16.9	16.49	16.66	0.48	78	51
4L	(1650°F/1/2 hr/AC) + (1100°F/8 hr/FC) to (932°F/120 hr)	130.0	120.5	20.0	31.0	15.5	14.65	14.78	0.48	54	28
4GB	(30% CR) + (1400°F/1 hr/AC)	131.0	119.9	17.0	52.0		17.23	18.43	0.30	111	51
4HA	(30% CR) + (1650°F/1 hr/AC)	125.7	111.9	16.0	45.0		13.40	13.55	0.30	89	37

Alloy & identification	Condition	UTS (ksi)	0.2% yield (ksi)	% along (in. / in.)	R.A. (%)	E (ksi × 10^3)	$P_{5\%}$ (kips)	P_{max} (kips)	Notch bend thickness (in.)	K_{Ic} (ksi $\sqrt{in.}$)	K_{Iscc}** (ksi $\sqrt{in.}$)
4IA	30% CR	152.6	134.8	13.0	43.0		11.75	11.75	0.30	74	47
4JA	30% HR at 1650°F	138.9	127.2	18.0	46.0		16.88	17.13	0.30	112	41
4KA	(30% CR) + (1100°F/8 hr/AC)	141.4	131.6	17.0	49.0		13.72	13.78	0.30	92	41

AC = Air cooled
WQ = Water quenched
CR = Cold rolled
HR = Hot rolled
FC = Furnace cooled

*Load determined from intersection of load-deflection curve and secant modulus having a slope 5% less than tangent modulus
**Threshold for loading in salt solution, except values in parenthesis are for loading in air and then adding salt solution

APPENDIX B

Strength, Toughness, and Stress-Corrosion Resistance
of $\alpha + \beta$ Titanium Alloys

Alloy & identification	Condition	UTS (ksi)	0.2% yield (ksi)	% elong (in 1 in.)	R.A. (%)	E (ksi x 10³)	$P_{5\%}$* (kips)	P_{max} (kips)	Notch bend thickness (in.)	K_{Ic} (ksi √in.)	F_{tscc} (ksi √in.)
Ti-2.25Al-1Sn-4Mo-0.2Si (IMI 680)	(2100°F Forge) + (1500°F/1/2 hr/WQ) + (930°F/24 hr/AC)	190.5	160.1	7	16	16.0	9.60	10.05	0.48	44	28
Ti-4Al-3Mo-1V (Ref.4)											
F11	1250°F/8 hr/AC	127.0	125.7	16	58		24.1	28.3	0.48	116	104
F24	(1875°F/1 hr/AC) + (1725°F/1 hr/WQ) + (1150°F/8 hr/AC)	154.8	137.2	7	16		20.4	21.7	0.48	96	77
Ti-4Al-4Mo-2Sn-0.5Si (Hylite 50)											
13A	1650°F/1/2 hr/WQ	169.4	136.0	16.5	46.5	15.1	11.08	11.08	0.48	56	44
13B	1800°F/1/2 hr/WQ	212.0	182.3	4.0	6.0	15.9	8.13	8.13	0.48	49	43
13C	(1650°F/1/2 hr/AC) + (932°F/24 hr/AC)	168.5	157.5	14.0	45.5	18.5	12.08	12.08	0.48	55	27
13D	(1650°F/1/2 hr/AC) + (1100°F/24 hr/AC)	162.7	153.7	14.0	44.0	17.7	9.03	9.03	0.48	44	23
13E	(1650°F/1/2 hr/AC) + (1300°F/24 hr/AC)	150.7	145.6	14.5	43.0	17.8	8.85	8.85	0.48	42	22
13F	(1500°F/1/2 hr/WQ) + (1100°F/24 hr/AC)	157.2	150.4	14.0	43.5	17.9	9.73	9.73	0.48	45	19
13G	(1650°F/1/2 hr/WQ) + (1100°F/24 hr/AC)	175.6	164.7	11.5	38.5	17.6	6.83	6.83	0.48	31	19
13H	(1800°F/1/2 hr/AC) + (1650°F/1/2 hr/WQ) + (1100°F/24 hr/AC)	172.6	156.8	5.0	7.5	17.6	12.99	13.09	0.48	62	31
13I	(1800°F/1/2 hr/AC) + (1650°F/1/2 hr/AC) + (932°F/24 hr/AC)	167.2	148.7	9.0	19.0		20.9	23.7	0.48	92	80
13JA	(1650°F/1/2 hr/AC) + (20% CR) + (932°F/24 hr/AC)	190.7	178.5	13.0	45.5	20.0	10.75	10.75	0.48	52	24
13JB	(1650°F/1/2 hr/AC) + (20% HR @ 932°F) + (932°F/24 hr/AC)	195.5	179.8	11.0	48.0	18.7	9.75	9.75	0.48	47	20
13K	(1650°F/1/2 hr/AC) + (1800°F/24 hr/AC) + (932°F/16 hr/AC)	176.5	168.5	16.0	51.9		16.0	16.9	0.48	75	26
13L	(20% CR) + (1650°F/20 min/AC) + (932°F/24 hr/AC)	125.9	152.2	15.0	59.0		15.1	15.2	0.48	72	36

24

Alloy & identification	Condition	UTS (ksi)	0.2% yield (ksi)	% elong (in 1 in.)	R.A. (%)	E (ksi x 10³)	P₅%* (kips)	P_max (kips)	Notch bend thick- ness (in.)	K_{Ic} (ksi √in.)	K_{Iscc} (ksi √in.)
Ti-5A1-3Mo-1V-2Sn (Ref. 22)											
W5	(1857°F/1/2 hr/AC) + (1725°F/1/2 hr/WQ) + (1100°F/8 hr/AC)	167.3	147.0	3	4		14.8	15.5	0.48	70	52
Z4	(1650°F/30 min/AC) + (1300°F/8 hr/AC)	130.5	126.3	16	49.5		17.6	21.6	0.48	80	80
Ti-6A1-2Mo (Ref. 22)											
— —	1975°F/1/2 hr/AC) + (1825°F/1/2 hr/WQ) + (1200°F/4 hr/AC)	153.5	138.6	8	14	18.2	20.5	.	0.48	94	63
— —	(1700°F/1/2 hr/AC) + (1300°F/8 hr/AC)	127.8	118.6	15	42	17.9	20.1	— —	0.48	92	55
Ti-6A1-4V (Ref. 4)											
D4	(1900°F/1/2 hr/AC) + (1725°F/1/2 hr/WQ) + (1230°F/8 hr/AC)	155.3	142.2	9	21		20.0	22.7	0.48	87	58
B2	1300°F/2 hr/AC	152.8	144.1	14	41		12.5	13.5	0.48	61	34
Ti-6A1-6V-2Sn (Ref. 21)											
	(1800°F/1/2 hr/AC) + 1625°F/1 hr/WQ) + (1200°F/4 hr/AC)	166.1	152.9	9	17.5		14.9	15.1	0.48	72	45
	1300°F/2 hr/AC	157.6	150.7	14.5	31.5		11.5	11.8	0.48	59	37
Ti-5A1-5Z-1W-0.2Si (IMI 684) (Ref. 29)											
	(1913°F/45 min/WQ) + (932°/24 hr/AC)	154.0	135.0**	14	25				0.39***	75	34

Alloy & identification	Condition	UTS (ksi)	0.2% yield (ksi)	% elong (in 1 in.)	R.A. (%)	E (ksi x 10³)	P₅% * (kips)	P_max (kips)	Notch bend thickness (in.)	K_Ic (ksi √in.)	K_Iscc (ksi √in)
Ti-7Al-2.5Mo											
27A	50% HR (1750°F)	147.5	135.5	13.5	36.5	19.45	11.8	11.8	0.48	65	45
27B	1675°F/1/2 hr/WQ	137.8	106.0	16.0	36.5	15.20	18.13	18.33	0.48	95	80
27C	1800°F/1/2 hr/WQ	161.1	133.1	10.5	26.0	16.40	16.90	16.90	0.48	93	73
27D	1650°F/1/2 hr/AC	139.6	127.1	---	--	----	19.47	19.8	0.48	96	65
27E	(1650°F/1/2 hr/FC) to (932°F/120 hr/AC)	135.9	122.6	..	--	..	15.10	17.70	0.48	74	44
27F	(1800°F/1/2 hr/WQ) + (1100°F/8 hr/AC)	166.6	151.9	12.0	25.0	18.60	10.05	10.05	0.48	52	37
27G	(1500°F/4 hr/WQ) + (700°F/120 hr/AC)	141.6	117.2	..	--	----	11.20	11.25	0.48	59	40
27H	(1900°F/1/4 hr/AC) + (1800°F/1/2 hr/WQ) + (1100°F/8 hr/AC)	158.4	134.8	5.5	8.5	18.0	14.75	14.75	0.48	72	43
27I	(30% CR) + (1400°F/1/2 hr/FC)	156.1	150.9	13.0	51.0	--	6.00	6.05	0.32	43	37
27J	(30% CR) + (1650°F/1/2 hr/FC)	139.9	133.4	18.0	50.0		9.9	9.9	0.31	71	37
27K	30% CR	160.9	143.1	13.0	57.0		11.63	11.63	0.31	83	61
Ti-7Al-4Mo (Ref. 21)											
	(1925°F/1/2 hr/AC) + (1650°F/1/2 hr/WQ) + (1250°F/4 hr/AC)	157.6	143.4	10.5	18		14.4	14.6	0.48	68	44
	(1750°F/1/2 hr/AC) + (1400°F/4 hr/FC)	154.0	145.1	16	43		6.7	6.7	0.48	32	23
Ti-8Al-1Mo-1V											
Mill anneal	1450°F/8 hr/FC	148.4	140.9	10	24				0.48	46	18

WQ = Water quenched
AC = Air cooled
CR = Cold rolled
HR = Hot rolled
FC = Furnace cooled

*Load determined from intersection of load deflection curve and secant modulus having a slope 5% less than tangent modulus
**0.1% proof stress
***Charpy specimen configuration

DOCUMENT CONTROL DATA - R & D

(Security classification of title, body of abstract and indexing annotation must be entered when the overall report is classified)

1. ORIGINATING ACTIVITY *(Corporate author)*	2a. REPORT SECURITY CLASSIFICATION
The Boeing Company Commercial Airplane Division Renton, Washington	Unclassified
	2b. GROUP

3. REPORT TITLE

Relationship Between Composition, Microstructure, and Stress Corrosion Cracking in Titanium Alloys

4. DESCRIPTIVE NOTES *(Type of report and inclusive dates)*

Research Report

5. AUTHOR(S) *(First name, middle initial, last name)*

R. E. Curtis

6. REPORT DATE	7a. TOTAL NO. OF PAGES	7b. NO. OF REFS
October 1968	26	29

8a. CONTRACT OR GRANT NO. N00014-66-C0365	9a. ORIGINATOR'S REPORT NUMBER(S)
b. PROJECT NO.	
c.	9b. OTHER REPORT NO(S) *(Any other numbers that may be assigned this report)* Boeing Document D6-23716
d.	

10. DISTRIBUTION STATEMENT

Reproduction in whole or in part is permitted by the United States Government. Distribution of this document is unlimited.

11. SUPPLEMENTARY NOTES	12. SPONSORING MILITARY ACTIVITY
	Advanced Research Projects Agency Department of Defense

13. ABSTRACT

Four α titanium alloys and 11 $\alpha+\beta$ titanium alloys have been characterized to relate phase composition and associated microstructure to stress corrosion cracking (SCC). Of these alloys, only a low-interstitial, commercially pure α alloy (Ti-50A) was immune to SCC. Addition of oxygen, aluminum, or aluminum and tin restricted slip in the α phase and promoted stress corrosion susceptibility. Formation of ordered domains of $Ti_3(Al, Sn)$ further restricted slip and increased susceptibility. Stress corrosion resistance was improved by thermomechanical treatments that reduced α grain size or increased dislocation density. Alpha-phase susceptibility is qualitatively related to the intensity of the stress field surrounding a dislocation pileup. Alloying with molybdenum and/or vanadium increased strength and often improved stress corrosion resistance. This is attributed to stabilization of the ductile β phase. However, precipitation of a fine dispersion of α or ω in β caused embrittlement and reduced the stress corrosion threshold. Intermetallic compound formation in alloys containing copper or silicon similarly promoted susceptibility. Thermomechanical processing of Ti-4Al-4Mo-2Sn-0.5Si limited the embrittlement, probably by refining Ti_5Si_3 particles in the β phase.

DD FORM **1473**

14. KEY WORDS	LINK A		LINK B		LINK C	
	ROLE	WT	ROLE	WT	ROLE	WT
Stress Corrosion						
Titanium Alloys						
Microstructure						
Composition						